Chromium (VI) and nickel removal by resin supported nanomagnetite: column experiments

MYSTRIOTI C.[1*], PAPASSIOPI N.[1], XENIDIS A.[1*]

[1]School of Mining and Metallurgical Engineering, National Technical University of Athens, 15780, Greece

*corresponding author: e-mail: chmistrioti@metal.ntua.gr

Abstract
Magnetite is a mixed-valent iron oxide with magnetic properties, which is considered as an efficient adsorbent for the removal of Cr(VI) from the aquatic environment. However nanomagnetite possesses difficulties for in situ remediation applications due to clogging effects and high separation cost. For this reason a nanocomposite material consisting of nanomagnetite supported on a cation exchange resin, denoted as $R-nFe_3O_4$ was synthesized and was evaluated for chromates and nickel removal from contaminated waters under flow conditions. A column test was carried out using a glass column, with 1.80 cm internal diameter and ~7 cm length. The column was filled with 12.1 g of resin supported nanomagnetite. The efficiency of $R-nFe_3O_4$ was examined for mixed polluted streams with 1.25 mg L^{-1} concentration for both hexavalent chromium and nickel. The experiment was carried out using NaCl as background electrolyte and the pH of feed solution was around 3. The total amount of reduced Cr(VI) was equal to 10 mg, while the total amount of removed Ni was 20.2 mg. The adsorption of Cr(VI) was described by the Bohart–Adams kinetic model and the adsorption capacity per unit volume of sorbent bed was found equal to 690 mg/dm^3.

Keywords*: nanomagnetite, cationic resin, flow conditions, column tests, Cr(VI) removal.

1. Introduction

Iron oxides are highly promising materials because they can be used for a wide range of applications. Specifically, magnetite (Fe_3O_4) due to its size (nanoscale) exhibits superparamagnetic properties, which make it very attractive for several applications. Nanomagnetite can be applied in biomedicine as a drug carrier, as a contrast agent in magnetic resonance imaging, as useful material for catalysts, and in electronic applications (Wallyn et al. 2019). Nanomagnetite particles have demonstrated superparamagnetic behavior, making them ideal absorbent materials for processing polluted waters due to their effective separation from water using a magnetic field (Goya et al. 2003, Aivazoglou et al. 2018). The properties of iron oxides (size, chemical composition, magnetic properties) are closely related to the method of their preparation, which determines the nucleation of nanoparticles. The most common method of synthesis is the chemical co-precipitation of Fe(III) and Fe(II) using a strong base such as ammonia or sodium hydroxide (Schwertmann and Cornell, 2000). This method requires high temperature and several hours of reaction until the formation of nanomagnetite (Schwertmann and Cornell 2000, Wallyn et al. 2019).

Particles of magnetite were examined in this study for their binding to ion exchange resin in order to investigate the effectiveness of magnetite under continuous flow conditions for the purification of water contaminated with low levels of hexavalent chromium and nickel. Binding of the magnetite to an inert substrate was necessary to avoid problems of agglomeration and pore blocking of the pure nanomagnetite.

2. Materials and Methods

2.1. Synthesis of R- R-nFe

The process of incorporating magnetite into cationic resin consists of three synthesis stages. The first stage involves the partial reduction of Fe(III) to Fe(II) by the addition of elemental iron in small quantities. The experimental procedure for the first stage initially involves weighing 13.5g of $FeCl_3\bullet6H_2O$ and dissolving it in 150 mL of deionized water in a 500mL capacity glass beaker. To the solution of trivalent iron, 25mL of 2M HCl is added, and the solution is finally brought to a final volume of 250 mL. Subsequently, the solution is transferred to a spherical reactor with a capacity of 500 mL, and 0.44g of Fe(0) is introduced. The solution is stirred at 300 rpm for two hours to obtain a final concentration of Fe(III) of 0.15mol/L and Fe(II) of 0.075mol/L. After the two hours, the solution is separated from the elemental iron. The second synthesis stage involves mixing 27.5g of Amberlyst 15 resin, which is placed in a 0.5L capacity conical flask together

with the solution obtained from stage 1. The solution is stirred for 2 hours to allow iron to be absorbed into the resin. After 2 hours, the resin is separated and washed with 1L of deionized water to remove any water-soluble iron. In the third stage, the resin (27.5g from stage 2) is mixed with 100mL of 3.5mol/L NaOH solution, and the nanomagnetite is formed. The amount of nanomagnetite incorporated in the resin, denoted as R-nFe$_3$O$_4$, is estimated to be equal to 53 mg per gram of resin. The R-nFe$_3$O$_4$ nanoparticles were characterized by X-ray diffraction and scanning electron microscopy (SEM).

The effectiveness of the nanostructured material R-nFe$_3$O$_4$ was evaluated by a continuous flow test in a column. The detailed properties of the column are given in Table 4.5. The experiment was conducted using HPLC glass columns with an inner diameter of 1.8 cm and a length of approximately 10 cm. The columns were filled with approximately 12.09 g of R-nFe$_3$O$_4$, which occupied a volume of 17.81 mL. The material was placed in layers and gently vibrated at various stages to ensure its uniform placement. The apparent density of the columns ranges from 0.68 g/cm^3. The columns were connected to a peristaltic pump and to the feed tank containing the solution. The tank was maintained under an inert nitrogen atmosphere. Initially, the column was fed with 1.5L of a solution of sodium chloride with a concentration of 0.02 M and a pH of 3 in order to remove the excess alkalinity of the resin with nanomagnetite. The alkalinity was due to the process of synthesizing the resin with nanomagnetite. Subsequently, the column was fed with polluted water containing weak concentrations of chromium and nickel and the effectiveness of R-nFe$_3$O$_4$ was studied under continuous flow conditions. Specifically, the feed solution contained 1.25 mg/L Cr(VI), 1.25 mg/L Ni, and 0.02 M NaCl as background electrolyte.

Table 1. Column properties

Parameters	R-nFe$_3$O$_4$
Resin mass, M (g)	12.09
Column diameter, d (cm)	1.8
Bed hight, L (cm)	7.0
Bed volume, BV (mL)	17.81
Particle density, ρ_P (g/cm^3)	1.21
Bulk density, ρ_b (g/cm^3)	0.68
Porosity, θ [c]	0.44
Pore volume, V_{PV} (cm^3) [d]	5.02
Flow, Q (cm^3/min)	1
Pore velocity, v (cm/min) [e]	0.9

Sampling at the column effluents was daily and samples were analyzed for pH, EC, Cr(VI) concentration, total

chromium, iron and nickel concentration. Total chromium, iron and nickel analysis were performed on ICP-OES. Hexavalent chromium was analyzed using USEPA Method 7196a.

3. Results

The X-ray diffraction patterns of the resin as it is and the R-nFe$_3$O$_4$ are presented in Figure 1. The X-ray diffraction pattern of the resin does not show any peaks. On the other hand, the X-ray diffraction pattern of R-nFe$_3$O$_4$ exhibits a significant change upon the incorporation of the nano-magnetite, with the appearance of the characteristic peaks of magnetite (220, 311, 400, 511, and 440).
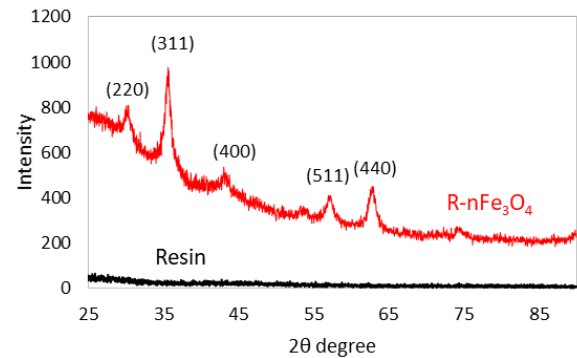

Figure 1. XRD patterns of resin and R-nFe$_3$O$_4$

The results of SEM and EDS analysis demonstrated that the nanomagnetite was supported in resin beads and the Fe concentration was equal to 7.23%. The iron was uniformly distributed at the resin beads.

The initial concentration of Cr(VI) in the feed solution was 1.25 mg/L. The flow rate corresponded to a contact time (τ) equal to 6 minutes. The evolution of Cr(VI) concentration in the outflow of the column is given in Fig. 2.
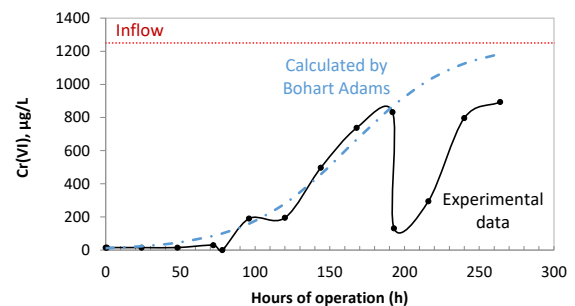

Figure 2. Cr(VI) evolution in the outflow of the column

Detectable concentrations of Cr(VI) were recorded after 78h. The concentration fluctuations observed in the breakthrough curve are due to the weekend shutdowns. This change in concentration is related to the increase in the residence time of the solution in the bed of nanomagnetite. In Fig. 2. the breakthrough curve of hexavalent chromium and the curve based on the Bohart-Adams model are compared. The model appears to follow the column experimental data very accurately, until the shut-down event.

The Bohart–Adams model is oftenly used to describe breakthrough curve in column experiments. The model results in a linear form of equations, which facilitates the determination of their basic parameters, with the method of linear regression. The Eq. 1 from Bohart-Adams model is given below.

$$\ln\left(\frac{C_0}{C} - 1\right) = \frac{k_{BA}N_0Z}{u} - k_{BA}C_0t \qquad (1)$$

Where C_0 is the initial Cr(VI) concentration, C is the concentration of effluent at time, k_{BA} is the Bohart-Adams rate constant ($cm^3/(mg\cdot min)$), N_0 is the adsorption capacity of the adsorbent (mg/cm^3), u is the Darcy velocity and Z is the column height (cm).
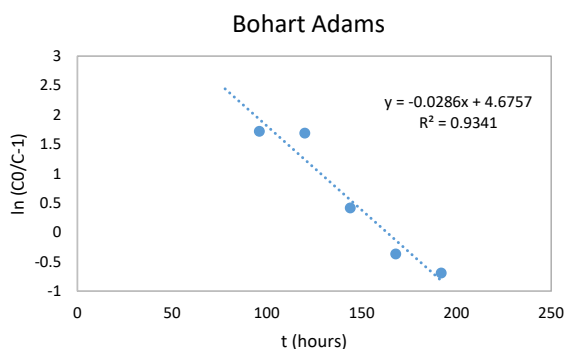

Figure 3. Linear regression of $\ln\left(\frac{C_0}{C} - 1\right)$ versus time in the column experiment.

The data were fitted to Bohart- Adams model in order to determine the values of both N_0 and k_{BA} which were calculated from the intercept and slope of a plot of $\ln\left(\frac{C_0}{C} - 1\right)$ against t as shown in Fig. 3. It has good fitting with R^2 value equal to 0.93 indicating that the model has good applicability.

Ni concentrations at the outflow of the column were lower than the detection limit of 40 μg/L throughout the column operation. Nickel is adsorbed on the cationic resin and on nanomagnetite. In total the column treated the equivalent of 926 bed volumes of the mixed Ni and Cr(VI) solution with initial concentration 1.25 mg/L, and was loaded with 1.13 mg of nickel per cm^3 of resin bed after 12 days of operation. The adsorption of Cr(VI) was described by the Bohart–Adams kinetic model and the adsorption capacity per unit volume of sorbent bed was found equal to 690 mg/dm^3. The concentration of iron in the effluent samples was less than 0.1 mg/L throughout the continuous flow test.

Table 2. Comparison of R-nFe_3O_4 performance for Cr(VI) removal with published data

Type	Adsorption capacity (mg/g)	Reference
Magnetite	14	[Hu et al. 2005]
Mixture magnetite, maghemite	6	[Chowdhury and Yanful 2010]
HA-Magnetite	3.4	[Jiang et al. 2014]
Magnetite	11.4	[Mystrioti et al. 2022]
Mixture magnetite, maghemite	17.4	[Mystrioti et al. 2022]

Taking into consideration the amount of incorporated nanomagnetite, 53 mg/g, the removal of Cr(VI) is equivalent to 19.2 mg Cr(VI) per gram of nFe_3O_4, which is a high performance in comparison with relevant published data (Table 2.)

4. Conclusion

In this study, the synthesis of R-nFe_3O_4 particles supported on a cation exchange resin was evaluated for nickel and chromate removal under flow conditions. The R-nFe_3O_4 particles were very effective for nickel as 16.5 L of mixed solution was treated. For the hexavalent chromium, the adsorption capacity was equal to 690 mg Cr(VI) per dm^3 of R-nFe_3O_4 bed volume.

References

Aivazoglou E., Metaxa E., Hristoforou E. (2018) Microwave-assisted synthesis of iron oxide nanoparticles in biocompatible organic environment. *AIP Adv.*, **8**, 48201.

Chowdhury S.R., Yanful E.K. (2010) Arsenic and chromium removal by mixed magnetite maghemite nanoparticles and the effect of phosphate on removal *J. Environ. Manage.* **91** 2238-2247.

Goya G.F., Berquó T.S., Fonseca F.C. (2003) Static and dynamic magnetic properties of spherical magnetite nanoparticles. *J. Appl. Phys.* **94**, 3520.

Hu J., Chen G. Lo I.M.C. (2005) Removal and recovery of Cr(VI) from wastewater by maghemite nanoparticles *Water Res.* **39** 4528–4536.

Jiang W., Cai Q., Xu W., Yang M., Cai Y., Dionysiou D.D. (2014**)** Cr(VI) Adsorption and Reduction by Humic Acid Coated on Magnetite. *Environ. Sci. Technol*. **48**, 8078−8085.

Mystrioti C, Papassiopi N, Xenidis A. (2022) Synthesis of Iron Nanomaterials for Environmental Applications from Hydrometallurgical Liquors. *Minerals*, **12** (5):556.

Schwertmann U., Cornell R. (2000) Iron Oxides in the Laboratory WILEY-VCH Verlag: Weinheim, Germany.

Wallyn J., Anton N., Vandamme T.F. (2019) Synthesis, Principles, and Properties of Magnetite Nanoparticles for In Vivo Imaging Applications—A Review. *Pharmaceutics*, **11**, 601.